A new experimental and analytical study of fully grouted rockbolts

Laura Blanco Martin, Faouzi Hadj Hassen, Michel Tijani, Aurélien Noiret

ARMA 11-242

A new experimental and analytical study of fully grouted rockbolts

BLANCO MARTÍN L., HADJ-HASSEN F., TIJANI M.
Department of Geosciences, MINES-ParisTech. 35, rue Saint-Honoré - 77305 Fontainebleau, France
NOIRET A.
ANDRA- Laboratoire de Recherche Souterrain de Meuse/Haute-Marne, RD 960, BP 9 - 55290 Bure, France

This paper was prepared for presentation at the 45th US Rock Mechanics / Geomechanics Symposium held in San Francisco, CA, June 26–29, 2011.

ABSTRACT: This paper deals with fully grouted rockbolts, both for mining and civil engineering applications. Their mechanical behavior under tensile loads is reviewed theoretically and experimentally. As for the theoretical part, a new solution able to predict the full range behavior of a grouted bolt subjected to a pull-out test is explained. The originality of the new approach lies in the fact that the boundary conditions only concern the free end of the bolt. The experimental part consists of a wide pull-out test campaign performed in laboratory on deformed steel bars and on FRP rockbolts. These tests have been carried out using a new experimental bench, whose main assets will be described. The influence of several parameters such as the confining pressure, the bolt profile and the quality of the grouting material has been considered. The results of these tests will help in the derivation of a constitutive law for the rockbolt-grout interface. *In situ* pull-out tests conducted in ANDRA's URL in North-Eastern France to examine the performance of different bars have also been analyzed and compared to the laboratory-scale results.

1. INTRODUCTION

Rockbolts have been extensively used for the past 30 years as reinforcement elements. A rockbolt consists of a bar inserted in a borehole that is drilled into the surrounding soil or rock mass and anchored to it by means of a fixture. A rockbolt reinforcement system has four principal components [1]: the rock or soil, the reinforcing bar, the internal fixture to the borehole wall and the external fixture to the excavation surface (a plate and a nut in most cases). Such system is very efficient if used in one or several of the following applications [2, 3];

- Stabilization of blocky rock masses, provided the far end of the bolt is anchored to a stable zone;
- Rock confinement, contributing to the use of the broken rock belt to confine the stable rock mass;
- Improvement of the mechanical properties of the rock mass.

In addition, the easy installation and low cost of rockbolts compared to those of other reinforcement elements have contributed to their worldwide success [4].

Fully grouted rockbolts are able to support tensile, compressive, shear and bending loads. The current study focuses on their tensile behavior because it is very often encountered and furthermore it allows studying the load transfer mechanism between the rock mass and the reinforcement element. Experience throughout the world has shown that under tensile solicitations failure often takes place by debonding at either the bolt-grout interface or at the grout-rock interface, depending on which one is weaker: in fact, if a bolted rock mass tries to move, a load will be progressively transferred to the rod and a shear stress will develop consequently along the embedded length (see figure 1). As the shear strength of the interface is progressively reached, debonding will occur.

Since Freeman [5] monitored for the first time in the 1970s the loading process and the stress distribution along the embedded length of a fully grouted rockbolt, numerous studies aiming at a better understanding of the load transfer mechanism between the surrounding ground and the bar have been conducted. Such studies comprise field monitoring [6, 7], laboratory [8-11] and *in situ* testing [12-15], analytical approaches [11, 16-19] and numerical modelling [20-22]. They have undoubtedly contributed to a better comprehension of the mechanical behavior of grouted rockbolts, to better design techniques and to a reduction in costs. Nevertheless, some aspects such as the analytical prediction of the axial load and the axial slip generated in an anchored rockbolt and the influence of parameters like the bolt profile or the confining pressure need to be reviewed.

The work currently undertaken by the authors tries to improve the knowledge acquired through these past works. The bond-slip model and the basis of the new analytical solution are presented first. The new experimental bench designed to test fully grouted rockbolts and cable bolts is described later, and the results obtained on steel deformed bars and Fibre Reinforced Polymer (FRP) rockbolts are discussed. So far, the influence on the anchoring capacity of the confining pressure, the embedment length, the type and profile of the bolt and the quality of the grouting material has been investigated. From these results, a constitutive law for the failure interface is being constructed. At the same time, *in situ* pull-out tests [23] performed in ANDRA's (*Agence Nationale pour la gestion des Déchets RAdioactifs* [French Public Agency in Charge of the Management of Radioactive Waste]) Underground Research Laboratory are presented and the results are compared to those obtained in laboratory scale in equivalent circumstances (same rockbolt, same grouting material).

2. THE BOND-SLIP MODEL

The bond-slip model is the constitutive law of the interface between the rockbolt and the grouting material (or between the grouting material and the rock mass). It represents the local shear stress – shear slip relationship, $\tau(W)$, of the failure interface; thus it takes into account the debonding mechanism that occurs as the shear slip increases. A bond-slip model often consists of three parts: elasticity (*i.e.*, the interface is totally coupled), plasticity (a decoupling front starts to propagate from the point where the load is applied to the free end of the bolt) and a residual phase, that remains due to friction.

Such a constitutive law can be derived from pull-out test results, provided the tests are conducted under accurate conditions. At laboratory scale, this means that the embedment length should be short enough to ensure a uniform distribution of the shear stress along the anchored length (*i.e.*, the shear slip is the same at every point of the rockbolt). Since a rheological law is not dependent upon the length, it can be validated by conducting two pull-out tests under identical conditions but using two different embedment lengths. This fact has been taken into account in the experimental study presented in section 4.

The rheological characterisation of the joint interface proves to be interesting in the design of rockbolt reinforcement patterns (bolt dimensions and spacing, maximum and residual strengths and associated slips). The stress distribution in an elementary bolt length *dz* is shown in figure 1.

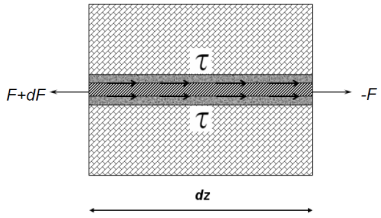

Fig. 1. Stress distribution in an elementary length *dz*.

As it can be inferred from the diagram, knowledge of the interface constitutive law allows predicting the load on the rockbolt according to Eq. (1):

$$dF = 2\pi R\,\tau(W)\,dZ \tag{1}$$

Regarding numerical modelling, such law permits a discretized approach, in contrast to classic homogenisation and reinforced-properties (namely, cohesion and friction angle of the rock mass) approaches.

3. ANALYTICAL APPROACH

A mathematical model able to predict the full-range behavior of a fully grouted rockbolt (in terms of axial force and axial displacement) subjected to a tensile load has been recently developed. It is limited to monotonic loading, which means that the axial displacement of every point of the bar must be an increasing function of time. The data needed for its application are: bolt radius R_b and length L, bolt's Young modulus E_b and the constitutive law of the rockbolt-grout (or rock-grout) joint interface, $\tau(W)$. The system equations and the resolution method are explained in detail in [24], where a complete development of the solution in the case of a tri-linear bond-slip model is also included. Therefore, only the most important features are mentioned here.

Let $W(Z,T)$ be the axial displacement of the rockbolt that is in front of point Z of the joint interface. The axial deformation of the rockbolt is $W' = \frac{\partial W}{\partial Z}$. The reference axis Z is fixed on the borehole wall, so that $Z=0$ corresponds to the far end of such joint and $Z=L$ corresponds to the point where the load is applied. The position $Z=kT$ (where k=0 if the bolt length is supposed infinite and k=1 otherwise) corresponds to the free end of the bolt throughout the pull-out process. At this point, the displacement is T.

Two hypotheses have been considered in the model:

- The bolt remains in the elastic range during the whole loading process;
- The relative displacement (shear slip) between the rockbolt and the grouting material equals the axial displacement of the rockbolt (*i.e.*, the axial deformation of the bolt is negligible).

Then, the constitutive equations of the rockbolt and the interface joint are respectively:

$$F = \pi R_b^2 \sigma_b = \pi R_b^2 E_b W' \quad (2)$$

$$\tau = S(W) \quad (3)$$

Combining the equilibrium Eq. (1) with Eqs. (2) and (3) the governing equation of the problem is:

$$W'' = \frac{2}{E_b R_b} S(W) \quad (4)$$

The problem consists therefore of finding the axial displacement W (as a function of Z) that solves Eq. (4). Boundary conditions are:

$$\begin{aligned} W(kT,T) &= T \\ W'(kT,T) &= 0 \end{aligned} \quad (5)$$

According to Eq. (2), F is calculated from W'; thus the axial response of the rockbolt during a pull-out test is completely characterised by $W'(L,T)$ and $W(L,T)$.

Compared to previous solutions [16, 18, 19] the innovation of the current approach consists in using boundary conditions that only concern the free end of the bolt (in the previous cases, one boundary condition concerned the point where the load is applied). The control parameter of the new model is the displacement T of this end.

The validation of this new approach has been carried out by comparing experimental results issued from both field and laboratory pull-out tests with the force-displacement relationship predicted by the new model. The results are in good agreement, as shown in figures 2a and 2b. The *in situ* test was performed on a 15.26 mm diameter threaded steel rockbolt grouted using epoxy resin. The embedment length was 5 m. A tri-linear bond-slip model was assumed for the bolt-grout interface. Regarding the laboratory situation, a 20 mm diameter deformed steel rockbolt was anchored over 100 mm using Lokset resin grout. The confining pressure was 5 MPa. In this case, a nonlinear function $\tau(W)$ including an exponential decay proved to give better results than a classic tri-linear function. Further comparisons will be provided in the next section.

4. EXPERIMENTAL STUDY

In order to clarify the mechanism of load transfer between the ground and the rockbolt, pull-out tests have been carried out within the context of this research program. They have been conducted both in the laboratory and *in situ*, and an attempt to relate the results (in terms of peak and residual shear strengths and slips) has been made.

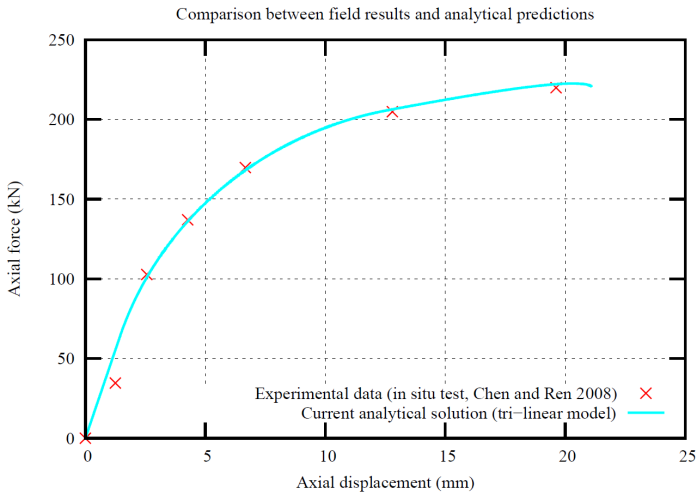

Fig. 2a. New analytical solution: comparison between a field pull-out test result and the theoretical prediction.

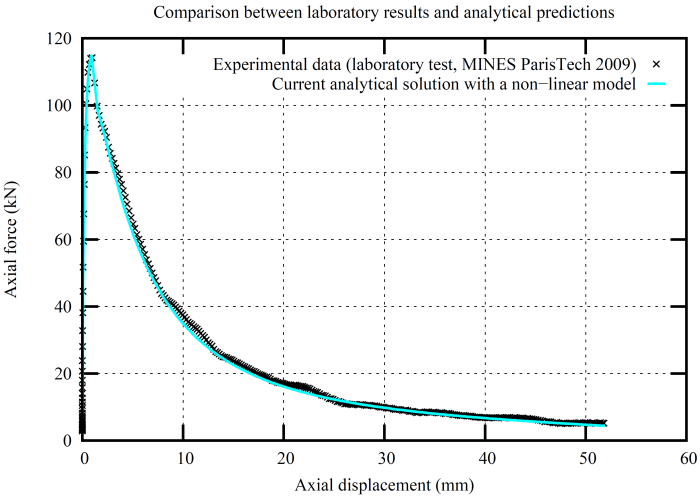

Fig. 2b. New analytical solution: comparison between a laboratory pull-out test result and the theoretical prediction.

4.1. *Laboratory investigation: equipment and procedure*

A new experimental bench has been designed and recently put into operation. Previous works [8-11, 25] have been considered during the design stage, so that improvements could be introduced in order to overcome some of the limitations encountered in the past. The main features of this new bench are described below.

The bench allows studying not only fully grouted rockbolts but also grouted cable bolts. Different grouting materials (resin, cementitious grouts) can be studied. The influence of the following parameters may be investigated: the confining pressure, the embedment length, the quality of the grout, the nature (type, profile) of the bolt, the roughness of the borehole surface, the influence of the thickness of the grout annulus and the rock sample tested.

Figure 3 shows a cutaway section of the current bench. The confining pressure may be maintained constant or

varied throughout the pull-out test; as a matter of fact, if the volume of confining oil is kept unchanged during the axial slip of the rockbolt, the effect of radial dilation can be studied. The axial force is applied via a 950 kN capacity & 70 mm stroke hollow ram jack and the axial displacement is measured using three LVDT sensors (the mean value is withheld). The force is measured using a 350 kN customized load cell. The tests are carried out under displacement control, using a constant displacement rate of 0.02 mm/s.

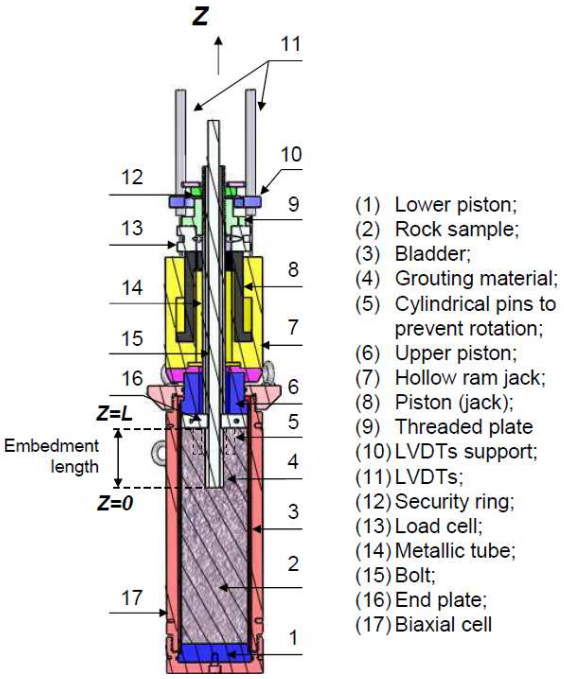

Fig. 3. Cutaway section of the new experimental bench.

Data are captured using LabVIEW. The acquisition frequency is 5 Hz. In order to study the residual capacity of the system (post-peak response), the bolts are normally pulled up to 70 mm.

As it can be seen in figure 3, the bench is based upon the double embedment principle: the bar length embedded in the rock mass represents the length where a debonding process might take place in a real situation, whereas the bolt length fixed to the metallic tube accounts for the fully anchored, load-carrying part. Thus in laboratory situations, no relative slip should take place inside the metallic tube. A highly resistant resin-based grout is used to anchor the rod to this tube.

It is important to note that, due to design considerations, the reaction force is made directly on the rock mass. As a result of the stress regime in the rock sample, a crater depression is likely to appear around the point where the bolt protrudes from the borehole. A comparison between tests where the crater formation took place and tests where it was prevented is presented in the following subsection. Since the main purpose of laboratory pull-out tests is to derive a constitutive law for the failure interface, such an end effect should be avoided in order to simplify the analysis and the interpretation of the results. For this reason, a metallic plate whose internal diameter matches the diameter of the tested bar has been designed. Once the constitutive law is determined, the tests where the crater depression occurred can be used to validate the new law by means of numerical modelling.

In the current research program, sandstone has been selected to be used as rock sample because of its good mechanical properties (see table 1), its homogeneity and also because it is a rock often present in coal mining environments (rockbolts and cable bolts are common support elements in gateroads for longwall mining).

One of the principal innovations of this bench consists in avoiding the well-known rotation phenomenon, especially in the case of cable bolts. Because of their low torsional rigidity due to their design (6 or more wires wound around a central *kingwire*), cables are likely to rotate under tensile loads. In fact, as the cable is progressively pulled out, it tends to "unscrew" from the grout imprints, which could cause the rock sample to rotate as well. To solve this matter, two actions have been undertaken: to prevent relative rotation between the rock sample and the jack, three dowel pins are inserted in three boreholes 10 mm long drilled in the rock sample, the end plate and the upper piston. At the same time, two dowels are inserted between the piston of the jack and the threaded plate, so that any possible relative displacement between the metallic tube and the hollow ram jack is blocked.

Table 1. Mechanical characteristics of the rock sample used

Property	Value
Young's modulus, E	25,600 MPa
Poisson's ratio, ν	0.26
Density, ρ	2140 kg/m^3
Uniaxial Compressive Strength, *UCS*	60 MPa
Tensile strength, R_t	3.1 MPa
Cohesion, C	12.4 MPa
Friction angle, φ	46º

4.2. Laboratory investigation: results

So far, 29 pull-out tests have been performed. Two types of rockbolts have been studied: steel HA25 deformed bars and FRP rockbolts. The nominal diameter of both rods is d_b=25 mm and their Young's moduli are 160,000 and 40,000 MPa respectively. The lateral surface of both bolts is ribbed: FRP rockbolts present a continuous standard thread (pitch length, l=10 mm; height of the asperities, h=1.5 mm), whereas HA25 bars are provided with a series of non-continuous annular ribs. The lateral surface of this bar is divided in two parts, so that one half presents parallel indentations and in the other half the ridges are laid following two different inclinations.

On average, l=16 mm and h=1.7mm. Figure 4 shows both bars.

Fig. 4. Profile of the rockbolts under study.

Six different confining pressures have been tested in order to take account of stress variation in field situations. Three anchoring lengths have been used: 90, 130 and 150 mm, which correspond to $3.6d_b$, $5.2d_b$ and $6.0d_b$ respectively. This choice has been recommended by other authors [8-11] to study the debonding process at the failure interface. Nonetheless, as announced in [12, 17], scatter of results is not negligible because of the short embedment lengths considered. Thus, tests should be carried out two or three times in identical conditions in order to confirm the results. With respect to the grouting material, Lokset SF resin and cementitious grouts (water:cement ratios, w:c=0.35 and w:c=0.40) have been tested. Table 2 compiles the characteristics of all the tests conducted.

After each pull-out test, the samples were cut and the interior was observed. In most cases, bond failure took place at the bolt-grout interface, see photographs 5a and 5b. Debonding at the rock-grout interface was also observed in some cases, especially when the borehole wall was not properly rifled, see figure 5c. Besides, the inspection of the samples has proved that the crater depression that is likely to appear around the mouth hole disrupts the debonding process along the embedment length, particularly when such length is short: as shown in photograph 5d, the failure planes in the grout are parallel to the failure plane in the rock sample.

The analysis of the pull-out tests conducted during the tuning phase of the experimental bench that took place at the beginning of this experimental research has indicated two interesting points: concerning the pull rate (at the beginning, some pull-out tests were performed at a rate of 0.8 mm/s), it has been observed that higher displacement rates privilege shearing off the grouting material between the indentations, especially when the bolt profile is rougher (HA25 rockbolts). The formation of gouge material confirms the considerable degradation at the bolt-grout interface. On the contrary, low pull rates favor a progressive damage of the joint interface. The

Table 2. Laboratory pull-out test campaign

Rockbolt	Confining pressure (MPa)	L(mm)	Grouting material
HA25	15	150	Resin
	10	130	Resin, w:c=0.35
		90	Resin
	5	130	Resin, w:c=0.40
		90	Resin
	2	130	Resin, w:c=0.35
		90	Resin
	1.2	130	Resin
		90	Resin
	0	130	Resin
		90	Resin
FRP	10	130	Resin
		90	Resin
	5	130	Resin, w:c=0.35
		90	Resin
	2	130	Resin, w:c=0.35
		90	Resin
	0	130	Resin
		90	Resin

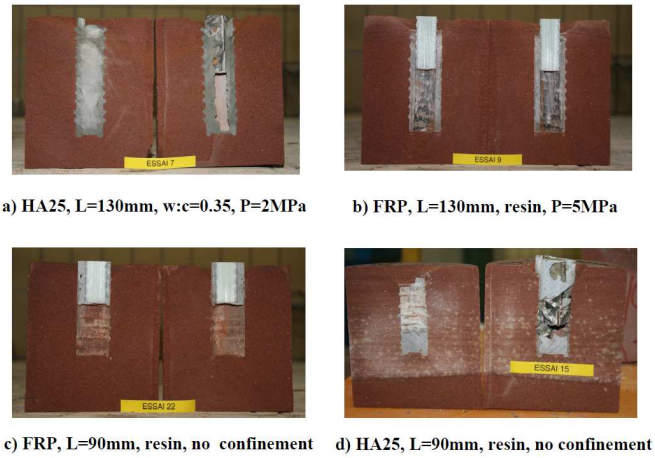

Fig. 5. Open view of some samples after the pull-out tests.

second point has to do with the crater depression: when this end effect propagates along the embedment length, the test results show important differences with respect to the tests where the embedded length is not disturbed. Figure 6 shows a comparison between two similar tests, except for the breakage of the grout during the pull-out process. As explained before, the altered tests will not be taken into consideration to derive a bond-slip model.

From the laboratory results, it has been concluded that the most influential parameter is undoubtedly the confining pressure: the peak load increases remarkably when the lateral pressure applied increases. The residual phase is also highly dependent on the confinement: when

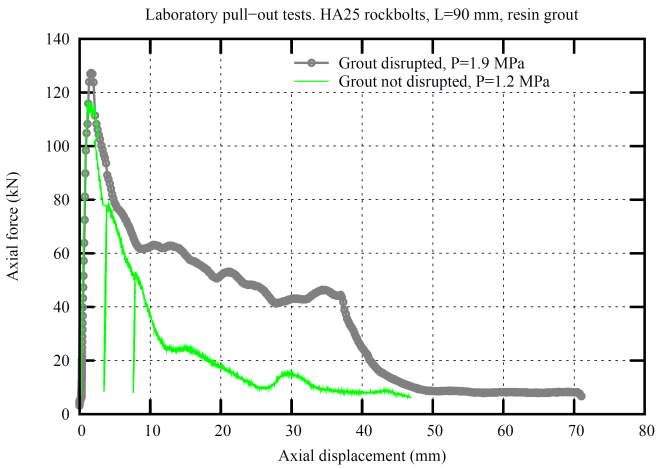

Fig. 6. Effect of the propagation of the crater effect along the anchored length.

the confining pressure is low, the profile of the bolt is likely to be well reproduced, so that the spacing between the peaks in the residual phase matches the distance between the bolt asperities. For higher confinements, the residual load switches towards a flat decrease. At the same time, as a result of the radial dilation developed (which decreases with lateral pressure), radial tensile cracks appear not only in the grout but also in the rock sample. As expected, the extension of these fractures is more important for lower confinements. Figure 7 accounts for the influence of the confining pressure on the axial response. The graphs show two tests conducted at confining pressures of 1.2 and 4.6 MPa respectively (the confinement is the only parameter that changes between the two tests). The bolt profile is almost absent when P=4.6 MPa. The figures below show the aspect of the grout and the rock sample after both tests; as it can be seen, radial fracturing is much more significant when P=1.2 MPa.

Moreover, if the volume of confining oil is maintained constant throughout the test, the increase in pressure can help in the calculation of the sample's dilation. For instance, in the case of FRP rockbolts, the confining pressure increased 1.5 MPa at the peak force when the initial confining pressure was 2 MPa, 0.5 MPa when the initial confining pressure was 5 MPa and only 0.3 MPa when the initial confinement was 10 MPa. As for HA25 rockbolts, the increase in the lateral pressure was less significant: less than 0.5 MPa for an initial confinement of 2 MPa. To further quantify the dilatant effect, pull-out tests have been planned on smooth steel bars.

As a final point, the comparison of two pull-out tests carried out under identical conditions but using two different embedment lengths is shown in figure 8. Several loading-unloading cycles have been executed. The initial slope is approximately 110 kN/mm in both cases and that of the cycles is 150 kN/mm. Even if these results suggest a proportional increase of the peak axial

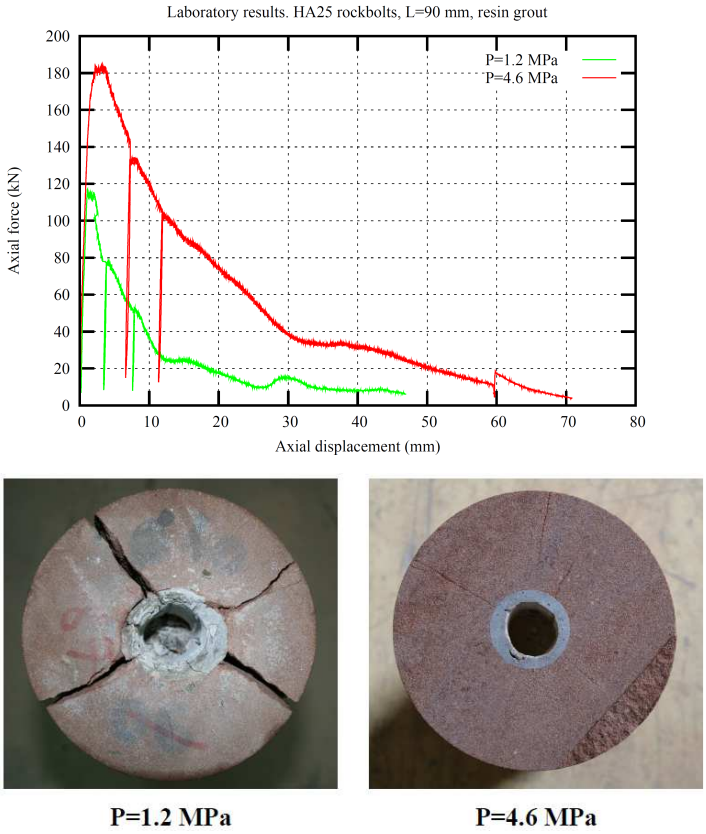

Fig. 7. Effect of the confining pressure on pull-out test results.

load with the embedment length, further tests are required before any conclusion is made.

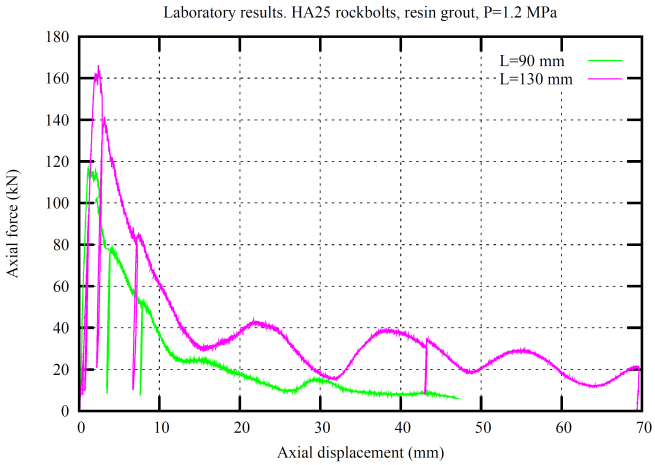

Fig. 8. Laboratory pull-out tests results. Influence of the embedment length.

4.3. In situ pull-out test campaign

Laboratory results should, as far as possible, be compared to real case situations where comparable conditions are met.

Within the framework of the ongoing excavation phase at ANDRA's Underground Research Laboratory (URL) located in Bure, 66 pull-out tests were performed in autumn 2009. They were carried out in two technical drifts, GT8 and GAT, oriented in the direction of the

maximum horizontal principal stress. Four types of rockbolts were tested: Swellex, CT-Bolts, HA25 and Dywidag 26WR. They were installed in the cross-sections between steel arches, with a radial layout. Since HA25 rockbolts have also been tested at laboratory scale, the comparison between laboratory and field results is limited to this type of bar. In the future, Dywidag 26WR continuous thread bars will also be tested in the laboratory and the results will be compared to those obtained *in situ*.

With regard to the operational conditions, the load was applied using a hollow ram jack and the displacement was measured using a potentiometer. It was decided that the tests would be carried out until either the axial load reached 90% of the yield strength of the bar, T_e, or the axial displacement reached 30mm.

Two types of tests were conducted according to the French Standards NF P 94-242-1 and NF P 94-153:

- Constant rate pull-out tests: the pull rate was comprised between 1 and 1.5 mm/min (0.02 mm/s on average);
- Creep tests: ten constant load levels ($\Delta F=10\%T_e$) were applied. The duration of each level increased with the applied load. The former levels lasted 15 minutes and the latter up to 1 hour.

Two grouting materials were used for HA25 rockbolts: Minova Lokset SF resin and a cementitious grout (w:c=0.5). The yield strength of these bars is 245 kN and that of the threaded part is 192 kN; therefore, the applied loads were in general lower than 173 kN. The anchored lengths tested were 2.4 and 3.0 m. Figure 9 shows typical constant rate pull-out tests results. The grouting material and the embedment length are indicated in each case. Four out of the five rockbolts were installed at the bottom of the sidewall; only the resin grouted rockbolt in the drift GT8 was located in the upper sidewall.

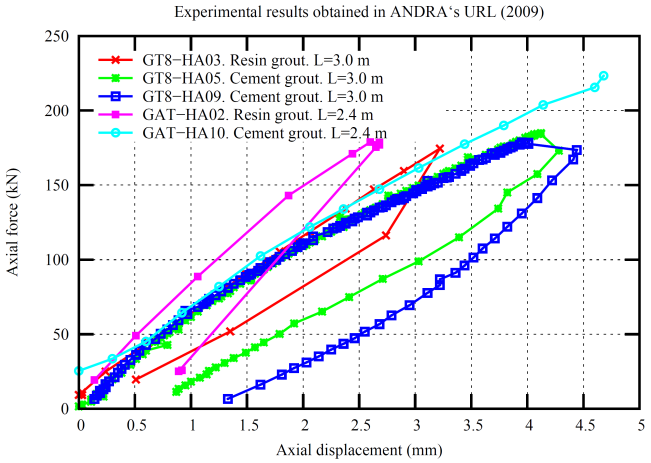

Fig. 9. *In situ* pull-out tests conducted in ANDRA's URL.

As a result of the long embedment lengths used, the tests were stopped at very low axial displacements, before any significant shear slip occurred. In some of them, the unload phase was also monitored, but there were no loading-unloading cycles. Besides, it can be inferred from the figure that the resin grouted rockbolts are more rigid than the cement grouted ones. The position of the bolt does not seem to have a major impact on the results. In terms of shear behavior, which was calculated according to [24] (since the lengths tested are quite important, it can not be assumed that the shear strength is uniformly distributed), the results for the same pull-out tests and their associated uncertainty are shown in figure 10. The solid lines account for the bond-slip models that best reproduce the experimental data and the error bars represent the possible models within an accuracy of ±5 % on the same data.

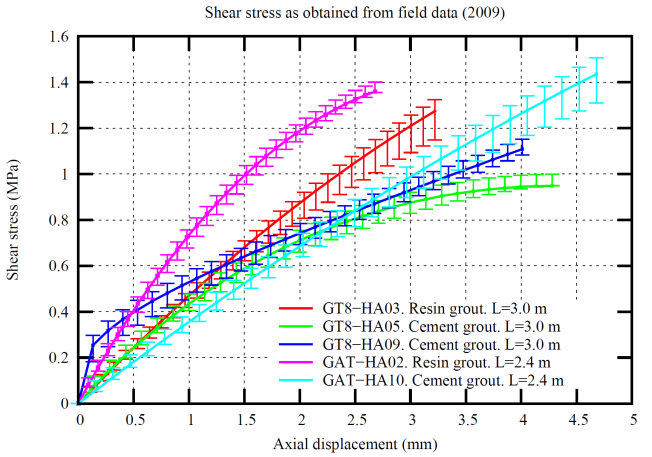

Fig. 10. Shear stress (and associated uncertainty) as derived from field pull-out tests.

The elastic stiffness of the $\tau(W)$ relationship is on average k_e=0.60 MPa/mm for the resin grouted bars and k_e=0.40 MPa/mm for the cement grouted bars. These values are consistent with previous field tests results [14], while a much larger stiffness (about 42.6 MPa/mm) was found in [15]. Moreover, it seems that the shear strength tends to a perfect plastic behavior characterized by a residual strength of about 1 MPa; nevertheless, in order to derive design information and to fully describe a bond-slip model as explained in [24], the axial slips should have been more important so that the debonding front would have been able to propagate all along the interface until the free end of the rockbolt. Anyway, the shear strength of a 0.5 w:c ratio grout can be calculated as stated in [26] using Eq. (6):

$$\tau_{peak} = 0.65 + 4.33\sqrt{\sigma_n} \qquad (6)$$

For the Lokset SF resin, the shear strength is around 25 MPa as reported in [27] (laboratory punched shear strength). These values are clearly higher than the maximum stresses reached during the pull-out tests,

which means that failure will possibly take place at the interface and not in the materials themselves.

Figure 11 compares the experimental data in figure 9 with the predicted axial load – axial displacement behavior obtained using the new analytical approach and the above bond-slip relationships. As it can be seen, the agreement is quite satisfactory.

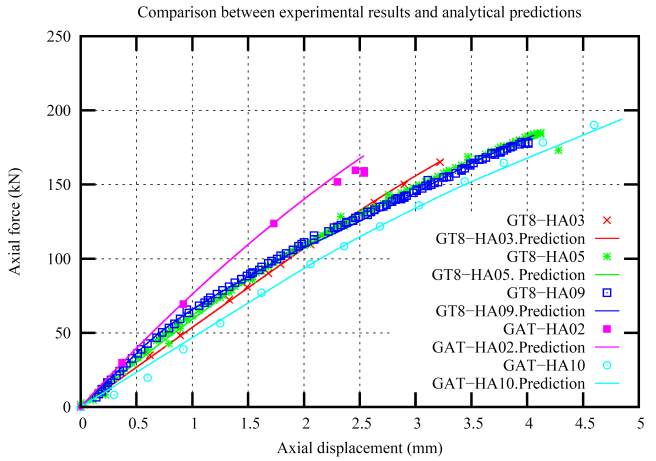

Fig. 11. New analytical solution: comparison between field experimental data and predicted results.

5. TOWARDS A CONSTITUTIVE LAW

From the laboratory results presented in section 4.2, a *τ(W)* relationship has been derived in each case. Taking into account the short embedment lengths tested, the shear stress has been derived according to Eq. (7):

$$\tau(W) = \frac{F(W)}{2\pi R(L-W)} \tag{7}$$

Even if the scatter in the results can not be neglected and some tests are less accurate than others, the general trend suggests a bond-slip model composed of an ascending branch followed by an exponential post-peak decay tending to a residual value. The use of two different embedment lengths for a same set of parameters permits to validate the shear strength – shear slip relationship, as it can be seen in figures 12 (FRP rockbolts) and 13 (HA25 rockbolts). Note that, in the blue curve in figure 12, the sudden drops in the shear stress that happen without a major change in the displacement are due to a substantial breakage of the grout during the pull-out test.

The values obtained are the same order of magnitude than those in [9]. The analysis of all tests discloses a rise of the shear stress up to a peak value for a small axial displacement (<6 mm), followed by a steep decay. The higher the confining pressure, the higher the peak strength, but the relationship is not linear. The displacement at which the peak takes place also increases with the confining pressure. It has been observed that the peak shear stress flattens at higher

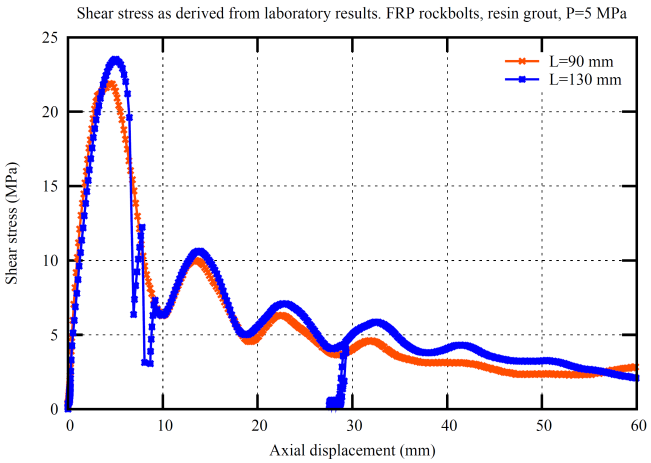

Fig. 12. Laboratory-derived shear stress - shear slip relationship. FRP rockbolts.

confinements, which is probably due to the decrease of dilation when the interface is sheared off. Concerning the initial linear stiffness, it has been found that it doesn't vary significantly for each type of rockbolt. It is about 14.5 MPa/mm for HA25 bars and 8.8 MPa/mm for FRP rods. The residual shear strength appears for a wide range of axial slips and is largely influenced by the evolution of the test (namely, breakage of the grout or the rock); in fact, the great scatter in the results can be explained by the variability that affects the parameters influencing the bond mechanism. As for the oscillations, their amplitude tends to decrease with the confining pressure. As expected, the wavelength is 16 mm for the steel rockbolts and 10 mm for the FRP bars.

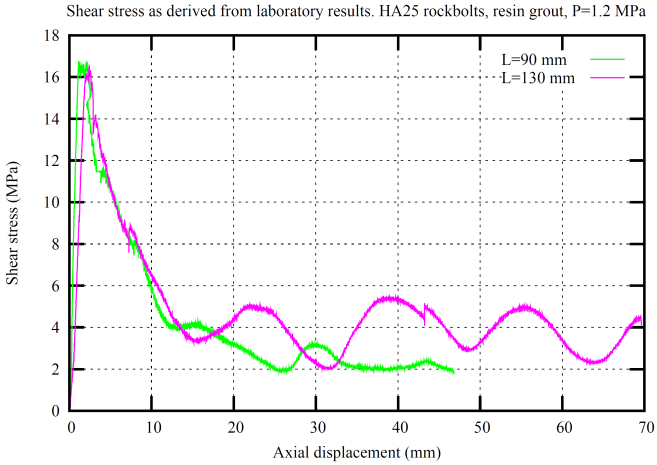

Fig. 13. Laboratory-derived shear stress – shear slip relationship. HA25 rockbolts.

With the intention of introducing the effect of the pressure in the constitutive law, the confinement has been varied during some tests while the axial displacement has been kept constant (constant embedment length conditions). So far, the pressure has been changed in the residual phase, *i.e.* for axial displacements beyond 50 mm. Figure 14 shows the dependence of the residual shear stress on the confining

pressure for two resin-grouted steel threaded bars. In the upcoming pull-out tests, the lateral pressure will be also varied at the peak load.

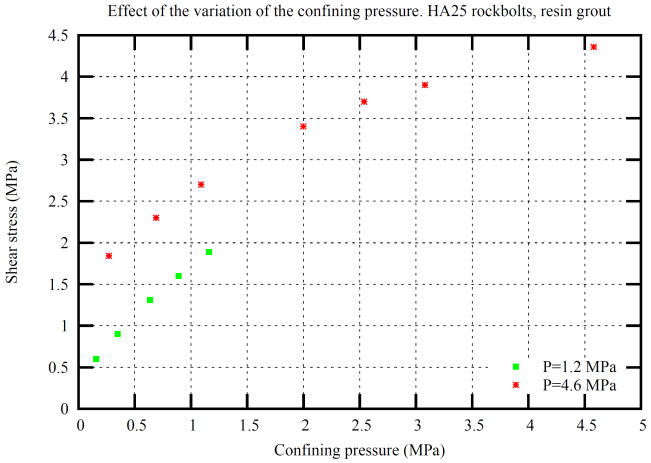

Fig. 14. Effect of the variation of the confining pressure on the shear stress. Residual phase, HA25 rockbolts.

Finally, as one could remark, the comparison between laboratory-derived and field-derived $\tau(W)$ relationships shows important differences; nevertheless, it is important to note that field and laboratory conditions may differ considerably: the rock sample properties and its degree of damage; the installation of the rockbolt (*in situ*, the plastic cartridges remain in the borehole, air bubbles are likely to form, etc., whereas in the laboratory the rockbolt is well centered in the borehole, the grouts are carefully prepared before being poured into the holes, …); the confining pressures applied in the laboratory, which may be rather higher than those in field (actually *in situ* stresses may vary considerably and this is difficult to reproduce at laboratory scale); the pull rate, and the scatter of the results also found in [14,15], among others.

6. CONCLUSIONS AND PERSPECTIVES

The failure mechanism by debonding of fully grouted rockbolts is reviewed theoretically and experimentally. Concerning the theoretical study, a new analytical solution that predicts the axial load – axial displacement response of a grouted bar is proposed. With reference to the experimental part, a laboratory scale pull-out test campaign is being carried out using a new experimental bench and the results are being analyzed. This campaign aims at the determination of a constitutive law for the rockbolt-grout or rock-grout failure joint interface. For this purpose, the influence of several parameters such as the confining pressure and the profile of the bolt is under study. Special attention is being paid to radial dilation, which develops as a result of the interface geometry and depends heavily on the confining pressure and on the strength of the grout and the rock. Laboratory and field pull-out tests results have been compared and an attempt to explain the differences encountered has been made.

The bond-slip model will be completed by the introduction of dilation and normal pressure and it will be implemented in a FEM code. Furthermore, a similar study will be carried out on classic seven strands and on modified geometry *Mini-Cage* cable bolts.

7. ACKNOWLEDGMENTS

This research is being undertaken in partnership with ANDRA. Rockbolts and grouting materials tested in the laboratory have been supplied by ANDRA, whose Research Department has kindly provided the authors with experimental *in situ* pull-out tests results. Funding and cooperation from partners within the framework of the European program RFCS (PROSAFECOAL Project) is also fondly acknowledged.

REFERENCES

1. Windsor C.R., and A.G. Thompson. 1993. *Rock reinforcement-technology, testing, design and evaluation. Comprehensive Rock Engineering* (Ed. J.A. Hudson). Oxford: Pergamon Press.
2. Chappell B.A. 1989. Rockbolts and shear stiffness in jointed rock mass. *Journal of Geotechnical and Geoenvironmental Engineering*: 115.
3. Fine J. 1998. In *Le soutènement des galeries minières*. Les Presses de l'Ecole des Mines de Paris. 199-220.
4. Stillborg B. 1986. *Professional Users Handbook for Rock Bolting* (Trans Tech Publications).
5. Freeman T.J. 1978. The behaviour of fully-bonded rock bolts in the Kielder experimental tunnel. *Tunnels and Tunnelling*: 37-40.
6. Choquet P., and F. Miller. 1988. Development and field testing of a tension measuring gauge for cable bolts used as ground support. *CIM Bulletin*. 81: 915: 53-59.
7. Health and Safety Executive. 2007. Guidance on the use of cable bolts to support roadways in coal mines. First published Caerphilly: 12/96.
8. Benmokrane B., A. Chennouf, and H.S. Mitri. 1995. Laboratory Evaluation of Cement-Based Grouts and Grouted Rock Anchors. *International Journal of Rock Mechanics and Mining Sciences*. 32: 633-642.
9. Moosavi M., A. Jafari, and A. Khosravi. 2005. Bond of cement grouted reinforcing bars under constant radial pressure. *Cement and Concrete Composites*. 27: 103-109.
10. Hagan P.C. 2004. Variation in load transfer of a fully encapsulated rockbolt. In *Proceedings 23rd International Conference on Ground Control in Mining*. Morgantown. Australia.

11. Hyett A.J., W.F. Bawden, G.R. Macsporran, and M. Moosavi. 1995. A Constitutive Law for Bond Failure of Fully-grouted Cable Bolts Using a Modified Hoek Cell. *International Journal of Rock Mechanics and Mining Sciences*. 32: 11-36.

12. Hyett A.J., W.F. Bawden, and R.D. Reichert. 1992. The Effect of Rock Mass Confinement on the Bond Strength of Fully Grouted Cable Bolts. *International Journal of Rock Mechanics and Mining Sciences*. 29: 503-524.

13. Rock Mechanics Technology Ltd for the Health and Safety Executive. 2004. *Coal mine roadway support system handbook*. Research Report 229a.

14. Chen W.W., and F.F. Ren. 2008. Mechanical behavior of the bamboo-steel composite rock-bolt. Report 2006BAK30B02. Dunhuang Academy & Cultural Relics Protection Center of Lanzhou University.

15. Rong G., H.C. Zhu, and C.B. Zhou. 2004. Testing study on working mechanism of fully grouted bolts of thread steel and smooth steel. Chin J Rock Mech Eng. 23(3): 469-475.

16. Farmer I.W. 1975. Stress Distribution along a Resin Grouted Rock Anchor. *International Journal of Rock Mechanics and Mining Sciences*. 12: 347-351.

17. Kaiser P.K., and S. Yacizi. 1992. Bond Strength of Grouted Cable Bolts. *International Journal of Rock Mechanics and Mining Sciences*. 29: 279-292.

18. Li C., and B. Stillborg. 1999. Analytical models for rock bolts. *International Journal of Rock Mechanics and Mining Sciences*. 36: 1013-1029.

19. Ren F.F., Z.J. Yang, J.F. Chen, and W.W. Chen. 2009. An analytical analysis of the full range behaviour of grouted rockbolts based on a tri-linear bond-slip model. *Construction and Building Materials*. 24: 361-370.

20. Larson H., T. Olofsson. 1983. Bolt action in jointed rock. In *Proceedings of the International Symposium on Rock Bolting, Abisko (Sweden), 28 August-2September 1983*, 33-46. Rotterdam: Balkema.

21. Fuller P.G., B.G. Hume, and R.G. Hume. 1996. Bolt load simulation and its practical application. *Rock mechanics*, eds. Aubertin, Hassani&Mitri, 187-193. Rotterdam: Balkema.

22. Ivanović A., and R.D. Neilson 2009. Modelling of debonding along the fixed anchor length. *International Journal of Rock Mechanics and Mining Sciences*. 46: 699-707.

23. ANDRA. 2009. *Essais de traction boulons d'ancrage. Campagne octobre 2009. Rapport des essais*. Report prepared by SOLDATA for ANDRA.

24. Blanco Martín. L., M. Tijani, and F. Hadj-Hassen. 2010. A New Analytical Solution to the Mechanical Behaviour of Fully Grouted Rockbolts Subjected to Pull-out Tests. *Construction and Building Materials*. 25: 749-755.

25. Rock Mechanics Technology Ltd for the Health and Safety Executive. 2006. *Testing and standards for rock reinforcement consumables*. Research Report 411.

26. Moosavi, M., W.F. Bawden. 2003. Shear strength of Portland cement grout. *Cement and Concrete Composites*. 25: 729-735.

27. Minova-Orica. 2009. *Lokset® Resin Capsules Product Data*. Minova Australia technical data sheet.